HEFAT2007
5th International Conference on Heat Transfer, Fluid Mechanics and Thermodynamics
Sun City, South Africa
Paper number: CH3

EFFICIENCY CALCULATIONS OF AIR-COOLED GAS TURBINES WITH INTERCOOLING

Canière H.*, Willockx A., Dick E. and De Paepe M.
*Author for correspondence
Department of Flow, Heat and Combustion Mechanics,
Ghent University - UGent,
St.-Pietersnieuwstraat 41, Gent, 9000,
Belgium,
E-mail: Hugo.Caniere@UGent.be

ABSTRACT

The working temperature of a gas turbine, necessary to achieve high efficiency, makes cooling of the first turbine stages unavoidable. Air and steam can be used for cooling. A model for an air-cooled gas turbine based on the work of Young and Wilcock [J.B. Young, R.C. Wilcock, ASME J. Turbomachinery 124 (2002) 207–221] is implemented in Aspen™. Simple cycle calculations with realistic parameters of current machines are made and confirm the results of Wilcock et al. [R.C. Wilcock, J.B. Young, J.H. Horlock, ASME J. Eng. Gas Turb. Power 127 (2005) 109–120] that increasing the turbine inlet temperature no longer means an increase in gas turbine cycle efficiency. This conclusion has important consequences for gas turbines because it breaks with the general accepted trend of increasing the TIT. An intercooled gas turbine cycle is intensively investigated, taking the turbine cooling into account. Intercooling not only lowers the work of compression, but also lowers cooling air temperatures. The major influences of the intercooling on the gas turbine cycle are mapped and explained. Optimum intercooling pressure for maximum gas turbine cycle efficiency is much lower than halfway compression. A simulation of the LMS100, the most recent gas turbine on the market from GE Energy, is made to verify the simulation methodology. The claimed intercooled cycle efficiency of 46% is confirmed. Further increasing the pressure ratio and TIT can still improve the performance of the intercooled gas turbine cycle.

NOMENCLATURE

A	[m²]	Surface area
Bi	[-]	Biot number
c_p	[J/kgK]	Specific heat capacity
FAR	[-]	Fuel/air ratio
h	[J/kg]	Specific enthalpy
H_u	[J/kg]	Lower heating value
K_{cool}	[-]	Cooling flow rate factor
m	[kg/s]	Mass flow rate
Q	[W]	Heat flux
p	[Pa]	Pressure
P	[W]	Power
r	[-]	Pressure ratio
s	[J/kgK]	Specific entropy
St	[-]	Stanton number
t	[m]	Thickness
T	[K]	Temperature
TBC		Thermal barrier coating
TIT	[°C]	Turbine inlet temperature
V	[m/s]	Velocity
W	[J/kg]	Specific work
α	[W/m²K]	Heat transfer coefficient
$\Delta\Sigma$	[J/K]	Entropy creation
ε_0	[-]	Total cooling effectiveness
$\varepsilon_{c,int}$	[-]	Internal flow cooling effectiveness
ε_f	[-]	Film cooling effectiveness
λ	[W/mK]	Thermal conductivity
η	[-]	Efficiency
ρ	[kg/m³]	Density

Subscripts

0	Total (against static) unit
$1, 2, 3$	Number of state
c, g	Coolant, main flow
k	State at compressor drain
m	Mechanical
met	Metal
s, r	Stator, rotor
w	Wall
x	State at mixing zone
*	At position of blade/vane

INTRODUCTION

During the last decades, gas turbine efficiencies were successfully improved by raising the compressor pressure ratio and the turbine inlet temperature (TIT). Advances in cooling technology and material science made high TIT possible. The challenge of constantly improving the gas turbine efficiency has reached a critical moment as Horlock et al. [1] investigated the limits of raising the combustor outlet temperature.

Maximum efficiency is suggested to be reached at TIT much lower than the stoichiometric combustion temperature due to the increase in losses associated with the cooling flows. Unless new materials and improved heat transfer mechanisms can restrict the increase in the necessary cooling air flow rates, it will not be worth raising the TIT much further. Wilcock et al. [2] made a detailed study on the gas properties as a limit on performance in the absence of cooling. It was shown that real gas effects are responsible for the peaks in cycle efficiency, even without cooling. Higher fuel/air ratios give higher water contents, which leads to higher values of specific heat capacities c_p and c_v. Wilcock et al. [3] made an overview of their investigations about the effect of the cooling on cycle efficiency. They conclude that improving allowable blade metal temperature and film cooling effectiveness are beneficial, but not as important as improving the turbomachinery aerodynamic efficiency.

In this work, a code based on the model of Young, J.B. and Wilcock, R.C. [4,5] has been implemented in Aspen™ [6]. Cycle calculations are made and the conclusions found by Wilcock et al. [3] are confirmed. GE's LMS100, a gas turbine with intercooling and the most recent machine on the market, reaches 46% efficiency [7,8], which is a major improvement. Therefore detailed investigations were made for gas turbine cycles with intercooling, mapping and explaining the major effects of the intercooler. Different from general cycle calculations (that include intercooling), turbine cooling has been taken into account, for intercooling not only lowers compression work, but also lowers cooling air flow rates due to lower cooling air temperatures.

THERMODYNAMIC MODEL OF AN AIR-COOLED GAS TURBINE

Cycle Scheme

In Figure 1 a model for an air-cooled gas turbine is represented. The compressor of the gas turbine is divided into 3 theoretical stages (C1-C3). After each of these stages cooling air can be tapped. Compressed air is heated in a combustion chamber with natural gas. Expansion takes place in 3 cooled turbine stages (T1-T3) and an uncooled turbine (T4). Each cooled turbine stage consists of a stator and rotor, cooled separately.

The compressors and the uncooled turbine are modeled as a polytropic compression process and a polytropic expansion process with given polytropic efficiency. The combustion chamber is modeled as a reactor where total combustion of natural gas takes place. The combustor outlet temperature (COT) is a design parameter. The fuel/air ratio (FAR) necessary to reach the desired COT is therefore determined. The combustor outlet temperature is set equal to the TIT. So, no heat losses are taken into account between the combustion chamber and the first stage of the turbine. A model for the air-cooled turbine stages is developed based on the work of Young and Wilcock [4,5]. The cooling flow rates, necessary to cool the blades, are estimated using the model of Holland and Thake [9]. The inlet air consists of N_2, O_2 and H_2O. The working fluid after combustion is assumed to be a mixture of N_2, O_2, CO_2 and H_2O. This model for an air-cooled gas turbine is implemented in Aspen ™ and gas properties are taken from the Aspen Properties ™ database [10].

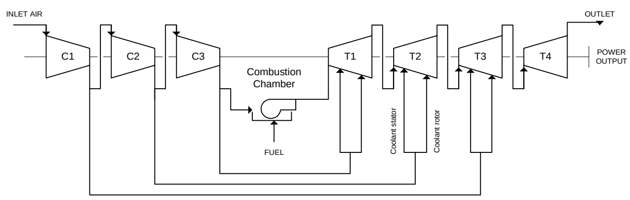

Figure 1 Scheme of air-cooled gas turbine

Model of cooled turbine stage

Contrary to the models with continuous cooled expansion (like the model of El-Masri [11] and De Paepe and Dick [12,13]), this model considers the expansion in separated turbine stages each divided in stator and rotor. At each turbine stage, 3 states are considered: the inlet state 1, the intermediate state 2 between stator and rotor and the outlet state 3. The coolant flow is first conducted through inner channels before being injected for film cooling. For simplicity, disk cooling implemented in the model of Young and Wilcock [5] is not adopted in the current model, because Young and Wilcock set the disk cooling flow at a fixed percentage of the main flow and no experimental verifications are available. The combustion pattern factor K_{comb}, which considers the temperature fluctuations after the combustor chamber and the type of combustor, is not implemented either.

The model is based on the first and second law of thermodynamics applied to stator parts: Eqs. (1)&(3), and rotor parts: Eqs. (2)&(4).

$$m_{g,1}\left(h_{0g,1}-h_{0g,2}\right)+m_{sc}\left(h_{0sc,k}-h_{0g,2}\right)=0 \tag{1}$$

$$m_{g,2}\left(h_{0g,2}-h_{0g,3}\right)+m_{rc}\left(h_{0rc,k}-h_{0g,3}\right)=P \tag{2}$$

$$\Delta\Sigma_s = m_{g,1}\left(s_{g,2}-s_{g,1}\right)+m_{sc}\left(s_{g,2}-s_{sc,k}\right) \tag{3}$$

$$\Delta\Sigma_r = m_{g,2}\left(s_{g,3}-s_{g,2}\right)+m_{rc}\left(s_{g,3}-s_{rc,k}\right) \tag{4}$$

When conditions of inlet air and coolant are known, state 2 after the stator can be calculated, if the entropy creation between state 1 and 2 (=$\Delta\Sigma_s$) is estimated. In Eqs. (2) and (4) the power output and state 3 are unknown, again assuming that $\Delta\Sigma_r$ can be estimated. This rotor system can be solved when the pressure at state 3 is known, by assuming the stage pressure ratio $r = p_1/p_2$. The cooling flow rates have to be estimated too. This will be explained in the next paragraph. A major assumption in the model is that the losses of the uncooled turbine are independent of the losses due to cooling. The uncooled turbine can be calculated as a polytropic expansion, with a polytropic efficiency. Supplementary losses due to cooling are implemented as entropy creating terms, as explained in detail by Young and Wilcock [4,5]. Submodels for friction losses, heat transfer losses and mixing losses are adopted and implemented.

Model for estimating cooling flow rates

The cooling flow rates required to cool the blades, are estimated using the model of Holland and Thake [9]. A scheme of the heat transfer model is shown in Figure 2. Parameters used in this model are:

- *internal flow cooling effectiveness* $\varepsilon_{c,\text{int}}$ (Eq. 5), which expresses the effectiveness of the heat transfer between the coolant air and the blade metal at the inside of the blades. Introducing this parameter one avoids to determine the heat transfer coefficient at the inside of the blade.

$$\varepsilon_{c,\text{int}} = \frac{T_{0c,x} - T_{0c,k}}{T_{met,\text{int}} - T_{0c,k}} \tag{5}$$

- *film cooling effectiveness* ε_f (Eq. 6), which expresses the effectiveness of the cooling achieved by creating a insulating film of coolant across the blade. T_{aw} is the mean adiabatic wall temperature, i.e. the temperature that would exist when no heat transfer through the blade is present.

$$\varepsilon_f = \frac{T_{0g} - T_{aw}}{T_{0g} - T_{0c,x}} \tag{6}$$

- *Biot numbers* of the metal Bi_{met} and the thermal coating TBC Bi_{tbc} (Eqs. 7-8), which include to the model the conduction through the thermal coating and the blade metal respectively.

$$Bi_{met} = \frac{T_{met,ext} - T_{met,\text{int}}}{T_{aw} - T_w} = \frac{\alpha_g t_{met}}{\lambda_{met}} \tag{7}$$

$$Bi_{tbc} = \frac{T_w - T_{met,ext}}{T_{aw} - T_w} = \frac{\alpha_g t_{tbc}}{\lambda_{tbc}} \tag{8}$$

- *total cooling effectiveness* ε_0 (Eq. 9). At maximum total cooling effectiveness, the cooling air heats up to the blade temperature.

$$\varepsilon_0 = \frac{T_{0g} - T_{met,ext}}{T_{0g} - T_{0c,k}} \tag{9}$$

- *cooling flow rate factor* K_{cool} (Eq. 10), which includes geometrical parameters and a Stanton number. The Stanton number, defined in Eq. (11) contains the convective heat transfer of the main flow.

$$K_{cool} = \frac{A_{surf}}{A_{g*}} \frac{c_{pg}}{c_{pc}} St_g \tag{10}$$

$$St_g = \frac{\alpha_g}{c_{pg} \rho_{g*} V_{g*}} \tag{11}$$

The main flow rate is defined in Eq. (12) with mean values ρ_{g*} for density, V_{g*} for velocity and A_{g*} for section. The external metal temperature $T_{m,ext}$ is set at the maximum allowable metal temperature $T_{max,ext}$ and is chosen as a design parameter. All other temperatures can be calculated when the total inlet temperatures are known.

$$m_g \approx \rho_{g*} V_{g*} A_{g*} \tag{12}$$

$$m_c = K_{cool} m_{c+} m_g \tag{13}$$

$$m_{c+} = \frac{m_c c_{pc}}{\alpha_g A_{surf}} = \frac{T_{aw} - T_w}{T_{0c,x} - T_{0c,k}} \tag{14}$$

The necessary cooling flow rates can be calculated with Eqs. (13-14). Typical values of the parameters used in the cycle calculations are shown in Table 1. They are based on the parameters used in Young and Wilcock [5].

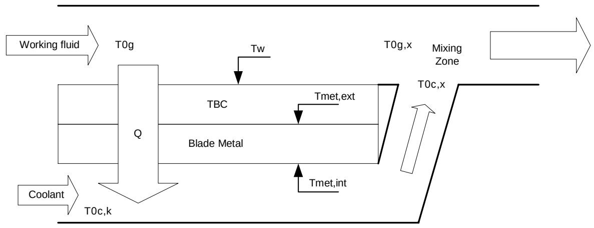

Figure 2 Scheme of heat transfer model

Table 1 Characteristic values of heat transfer model

Cooling flow rate factor K_{cool}	0.045
Internal cooling effectiveness $\varepsilon_{c,\text{int}}$	0.7
Film cooling effectiveness ε_f	0.4
Biot number metal Bi_{met}	0.15
Biot number TBC Bi_{tbc}	0.3
Maximum allowable blade temperature $T_{\max,ext}$	850°C

Results of simple cycle calculations

Cycle calculations are made in Aspen ™ based on the scheme of Figure 1. The major component characteristics are shown in Table 2. The pressure ratios of the compressors and the turbine stages are set to the ones of the GE LM6000.

$$\eta = \frac{W_{turbines} - W_{compressors}}{FAR \cdot H_u} \cdot \eta_m \tag{15}$$

Table 2 Characteristic values for cycle simulations

Polytropic compressor efficiency	92%
Polytropic turbine efficiency	92%
Combustion efficiency	99%
Mechanical efficiency	98%
Pressure drop combustion chamber	4%
Pressure drop inlet	0.01 bar
Pressure drop outlet	0.01 bar
Pressure drop intercooler	0 bar
Atmospheric conditions	1.013 bar, 15°C, $\varphi = 60\%$
Pressure ratio first compressor C1	1/3 r
Pressure ratio second compressor C2	3/5 r
Pressure ratio first turbine stage T1	2:1
Pressure ratio second turbine stage T2	2:1
Pressure ratio third turbine stage T3	2:1

The cycle efficiency η was calculated with Eq. (15), where $W_{turbines}$ is the specific work output of the turbines, $W_{compressors}$ the specific work input of the compressors and H_u the lower heating value, calculated by Aspen [TM] based on the combustion enthalpies of the gas components. In the cycle calculations, pressure, and so temperature, of the cooling air flows change with the pressure ratio.

Table 3 Simulation results compared to LM6000

	Specific power [kJ/kg]	Efficiency [%]	TOT [°C]
LM6000	345	41.5	452
Simulation	351	40.9	444

The simulation results are near to the test results of the LM6000, as shown in Table 3. The compressor and turbine efficiencies for the LM6000 were set to η_c=0.91 and η_t=0.90. There is a slight underestimation of the efficiency, although the simulation gives a higher specific power output. Simple-cycle calculations of the air cooled gas turbine model confirm the conclusions of Wilcock et al. [3]. As shown in Figure 3, there is a maximum in cycle efficiency for pressure ratio and TIT. For compressor and turbine efficiencies η_c=η_t=0.90, maximum efficiency is obtained for pressure ratios and temperatures used in current machines. The maximum moves to higher pressure ratios and lower TIT if higher polytropic efficiencies are used. The simulations give lower efficiencies than Wilcock et al. [3], but a numerical comparison is difficult to make because some simplifications of the turbine stage model are made. Furthermore, the model also includes the mechanical efficiency, pressure drops at inlet, outlet and combustion chamber and the combustion efficiency. Details about the configuration of Wilcock et al. are not published and a different property database is used.

The influence of the pressure ratios of the compressors, and thus the pressures of the cooling air, has been analyzed. It was found that these pressures do not significantly influence the efficiency. Therefore the conclusions about the efficiency found with the configuration of Figure 1 are valid for other configurations and thus can be generalized.

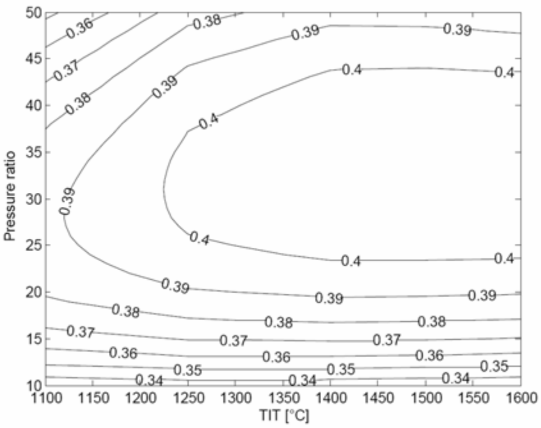

(a)

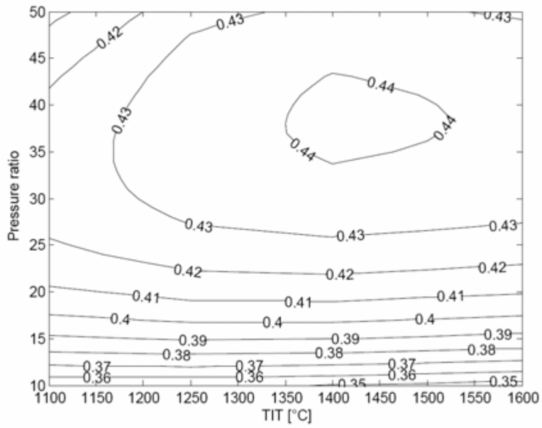

(b)

Figure 3 Efficiency of the simple cycle with (a) η_c=η_t=90% (b) η_c=η_t=92%

THERMODYNAMIC MODEL OF A GAS TURBINE WITH INTERCOOLING

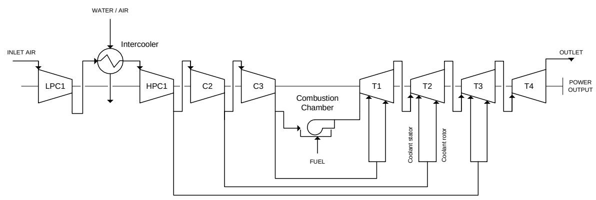

Figure 4 Scheme of gas turbine with intercooler

An extensive study of the effect of intercooling is made with the cycle scheme shown in Figure 4. Compared with the scheme shown in Figure 1, the first compressor C1 is split into two parts. The low pressure compressor LPC1 has pressure ratio $\sqrt{r}$. The compressed air after LPC1 is cooled with air or water. In a first series of simulations, the air is cooled to atmospheric conditions. This is an ideal case. The most recent machine on the market, GE's LMS100, has such an intercooler [7,8].

Intercooling has some positive and some negative effects on the efficiency, so again a maximum is expected. The major effect is the reduction of the work needed for compression and the lower temperatures of the cooling air. On the other hand, more fuel is needed to maintain the fixed TIT since energy is lost as heat in the intercooling.

Calculating the efficiency of the intercooled cycle, a maximum does not occur in the current region of r and TIT, but is to be expected for much higher pressures ratios and temperatures, i.e. the upper right corner of Figure 5. A significant improvement in efficiency can be reached when using high pressure ratios. This is an important conclusion for gas turbine manufacturers. A simulation of GE's LMS100 has been made as verification based on the data available [7,8]. An efficiency of 46% claimed by GE has been found. The pressure ratio of 42:1 in this machine is much higher than currently in use for machines of the same size (r = 28:1 for GE's popular

LM6000 machine). This has a positive effect on the efficiency (compared to the 41.5% efficiency of the LM6000).

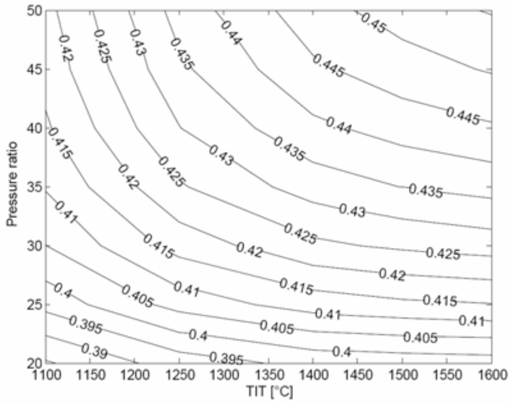

(a)

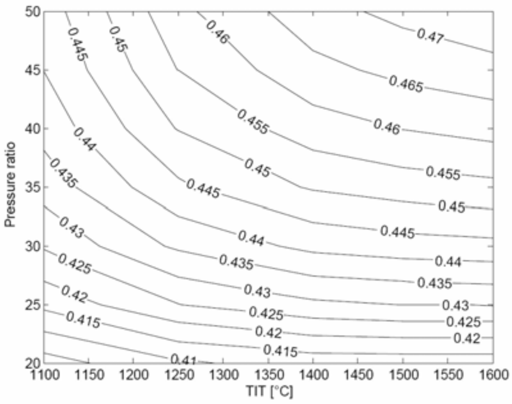

(b)

Figure 5 Efficiency of the intercooled cycle with (a) η_c=η_t=90% and (b) η_c=η_t=92%

The increase in efficiency is due to the increase in specific power output, being the difference between output and input power, as shown on Figure 6. This in turn can be explained by separating the effect of the compressors and the turbines. The work input needed for compression is lower due to the intercooler (Figure 7). The difference in work input compared to the simple cycle increases with the pressure ratio. Obviously, the work output of a turbine increases with the pressure ratio (Figure 8). Compared to the simple cycle, the output increase augments because less cooling air is needed in the intercooled cycle. This explains why the specific power increases compared to the simple cycle and why the increase in efficiency is higher with higher pressure ratios.

Adding intercooling means higher FAR, but the increase does not offset the increase in specific power. Moreover, the FAR decreases for increasing pressure ratio. According to the calculations, cooling flow rates do not increase much for increasing pressure ratio. Secondly, the effect of intercooling temperature has been analyzed. As expected, cooling to atmospheric temperature has the best result, i.e. a maximum intercooling effectiveness of 100%, but needs an infinitely large heat exchanger. In practice a compromise has to be made. At higher pressure ratios, the influence of the temperature after intercooling becomes more important as shown in Figure 9.

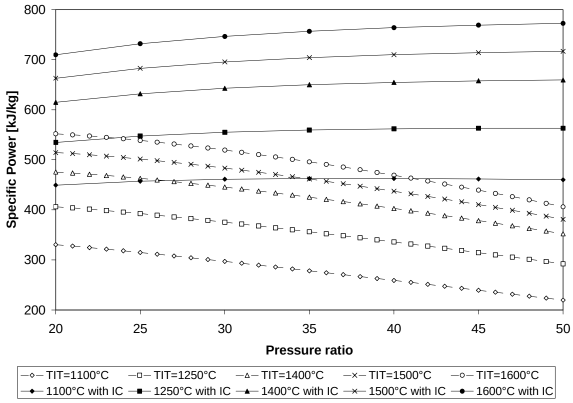

Figure 6 Specific power of cycle with intercooler

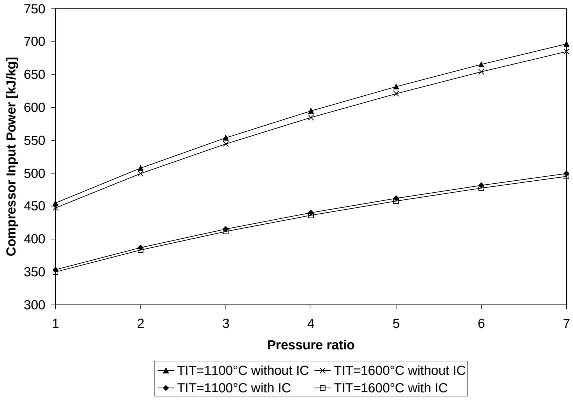

Figure 7 Compressor power of cycle with intercooler

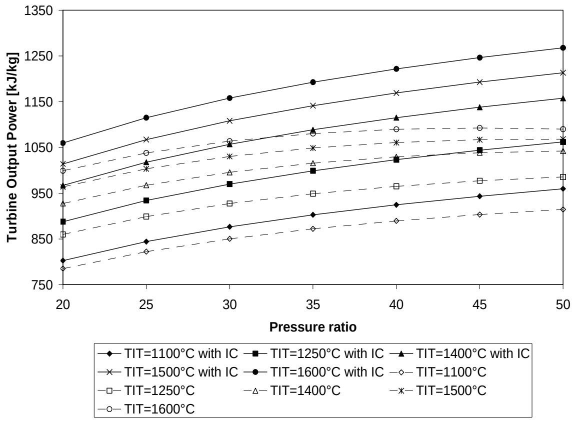

Figure 8 Turbine power of cycle with intercooler

The effect of intercooling pressure is more important than the intercooling temperature. Concerning only the work of the compressor, a minimum is reached halfway compression at:

$$p_{int\,ercooling} = \sqrt{\frac{p_{out}}{p_{in}}} \qquad (16)$$

But the intercooling pressure does not only influence the compressor work. So, the pressure in Eq. (16) does not give necessarily maximum efficiency of the intercooled gas turbine cycle. Lowering the intercooling pressure increases the compressor exit temperature, lowers the FAR, lowers the heat loss in the intercooler, but increases the cooling air temperature and so the needed cooling flow rate. Figure 10 shows the efficiency for varying pressure ratio of the intercooling. The resulting efficiency maximum is found at much lower intercooling pressure than calculated with Eq. (16). The difference in efficiency is about 2% for the studied case. It is important to mention that this conclusion is only true for the efficiency. Lowering the intercooling pressure changes the specific work output in a negative way. Concerning these effects, the simulation of the LMS100 reaches a perfect match. Even a higher efficiency than 46% has been found. Including practical losses, not concerned in the expansion model, the claimed efficiency can be reached.

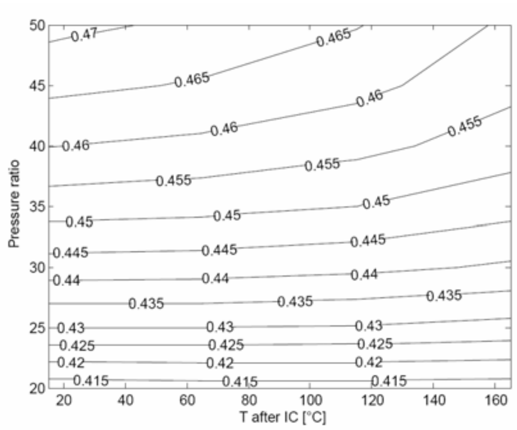

Figure 9 Efficiency of cycle with IC at TIT=1500°C for varying intercooling temperature

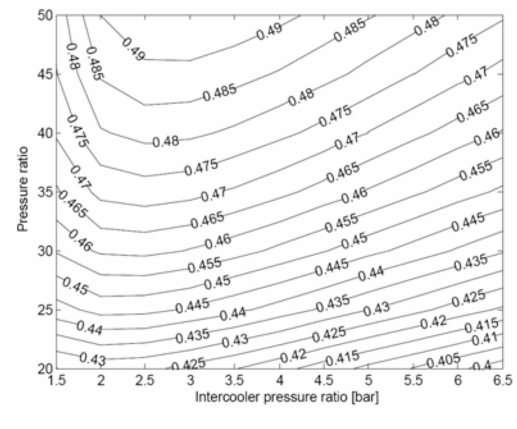

Figure 10 Efficiency of cycle with IC at TIT=1500°C for varying intercooling pressure ratio

CONCLUSION

Simulations of air-cooled gas turbines made with a model of Young and Wilcock [4,5] and implemented in Aspen TM, confirm the results of Wilcock et al. [3] that improved cycle efficiencies will not necessarily result from increased combustor outlet temperatures. The pressures of the cooling air do not significantly influence the efficiency, which makes calculations only weakly dependent on the pressure taps used in the model.

Calculations of a cycle with intercooler, including the effects of turbine cooling, prove the gain that can be made by using an intercooler combined with high polytropic efficiencies. The major influences of the intercooled gas turbine cycle were analyzed. The working pressure of the intercooler was investigated. Optimum intercooling pressure for maximum cycle efficiency is much lower than halfway compression. This corresponds with the position of the intercooler of the LMS100 machine of GE along the compression path. Further increase of TIT and pressure ratio can improve the efficiency of the cycle with intercooler.

REFERENCES

[1] Horlock J.H., Watson D.T. and Jones T.V., Limitations on Gas Turbine Performance Imposed by Large Turbine Cooling Flows, *ASME Journal of Engineering for Gas Turbines and Power,* Vol. 123, 2001, pp. 487-494.

[2] Wilcock R.C., Young J.B. and Horlock, J.H., Gas properties as a limit to gas turbine performance, *ASME Turbo-Expo 2002*, Amsterdam.

[3] Wilcock R.C., Young J.B. and Horlock J.H., The Effect of Turbine Blade Cooling on the Cylce Efficiency of Gas Turbine Power Cycles, *ASME Journal of Engineering for Gas Turbines and Power,* Vol. 127, 2005, pp. 109-120.

[4] Young J.B. and Wilcock R.C., Modeling the air-cooled gas turbine: Part 1 – General Thermodynamics, *ASME Journal of Turbomachinery*, Vol. 124, 2002, pp. 207-213.

[5] Young J.B. and Wilcock R.C., Modeling the air-cooled gas turbine: Part 2 – Coolant flows and losses, *ASME Journal of Turbomachinery*. Vol. 124, 2002, pp. 214-221.

[6] Aspen Plus TM, Software Package, Ver. 12.1, Aspen Technology Inc., Cambridge MA, USA, 2003.

[7] GE Power Systems, LMS100, GE's new gas turbine system: Designed to change the game in power generation, URL: http://www.gepower.com/prod_serv/products/aero_trubines/en/downloads/lms_brochure.pdf [cited 1 June 2005].

[8] Rahm S., Joshi N. and Kannel S., Why adding an LMS100 could improve the economic health of your coal plant, *Modern Power Systems*, December 2004/Janurary 2005, pp. 21-23.

[9] Holland M.J. and Thake T.F., Rotor Blade Cooling in High Pressure Turbines, *Journal of Aircraft*, Vol.17, 1980, pp. 412-418.

[10] Aspen Properties TM, Software package, Ver. 12.1, Aspen Technology, Inc., Cambridge MA, USA, 2003.

[11] El-Masri M., On thermodynamics of gas turbine cycles: Part 2 – a model for expansion in cooled turbines, *Journal of Engineering for Gas Turbines and Power,* Vol. 108, 1986, pp. 151-159.

[12] De Paepe M. and Dick, E., Cycle improvements to steam injected gas turbines, *International Journal of Energy Research*, Vol. 24, 2000, pp. 1081-1107.

[13] De Paepe M. and Dick E., Technological and economical analysis of water recovery in steam injected gas turbines, *Applied Thermal Engineering,* Vol. 21, 2001, pp. 135-156.